

REPORT DOCUMENTATION PAGE

Form Approved
OMB No. 0704-0188

The public reporting burden for this collection of information is estimated to average 1 hour per response, including the time for reviewing instructions, searching existing data sources, gathering and maintaining the data needed, and completing and reviewing the collection of information. Send comments regarding this burden estimate or any other aspect of this collection of information, including suggestions for reducing the burden, to the Department of Defense, Executive Services and Communications Directorate (0704-0188). Respondents should be aware that notwithstanding any other provision of law, no person shall be subject to any penalty for failing to comply with a collection of information if it does not display a currently valid OMB control number.

PLEASE DO NOT RETURN YOUR FORM TO THE ABOVE ORGANIZATION.

1. REPORT DATE (DD-MM-YYYY) 07-08-2008	2. REPORT TYPE Journal Article	3. DATES COVERED (From - To)		
4. TITLE AND SUBTITLE Advantages of Fine Resolution SSTs for Small Ocean Basins: Evaluation in the Black Sea			5a. CONTRACT NUMBER	
			5b. GRANT NUMBER	
			5c. PROGRAM ELEMENT NUMBER 0601153N	
6. AUTHOR(S) Birol Kara, Alan Wallcraft, Charlie Barron, Temel Oguz, K.S. Casey			5d. PROJECT NUMBER	
			5e. TASK NUMBER	
			5f. WORK UNIT NUMBER 73-5732-B7-5	
7. PERFORMING ORGANIZATION NAME(S) AND ADDRESS(ES) Naval Research Laboratory Oceanography Division Stennis Space Center, MS 39529-5004			8. PERFORMING ORGANIZATION REPORT NUMBER NRL/JA/7320--07-8016	
9. SPONSORING/MONITORING AGENCY NAME(S) AND ADDRESS(ES) Office of Naval Research 800 N. Quincy St. Arlington, VA 22217-5660			10. SPONSOR/MONITOR'S ACRONYM(S) ONR	
			11. SPONSOR/MONITOR'S REPORT NUMBER(S)	
12. DISTRIBUTION/AVAILABILITY STATEMENT Approved for public release, distribution is unlimited				
13. SUPPLEMENTARY NOTES 20080815 248				
14. ABSTRACT This paper examines monthly variability of climatological mean sea surface temperature (SST) in the Black Sea. A total of eight products, including observation- and model-based SST climatologies, are formed and compared with each other. Some of the observation-based SST data sets include only satellite measurements, while others combine in situ temperatures, such as those from moored and drifter buoys, with satellite data. Climatologies for numerical weather prediction (NWP) model-based data sets are formed using high temporal resolution (6 hourly) surface temperatures. Spatial resolution of these SST products varies greatly (\approx 4 km to 280 km), with the observation-based climatologies typically finer than the NWP-based climatologies. In the interior, all data sets are in general agreement, with annual mean SST biases typically within $\pm 0.2^{\circ}\text{C}$ in comparison to the finest resolution (4 km) satellite-based Pathfinder climatology. Major differences are near the land-sea boundaries where model-based SSTs pose serious biases (as much as $>5^{\circ}\text{C}$). Such errors are due to improper contamination of surface temperatures over...				
15. SUBJECT TERMS SST, climatology, Black Sea				
16. SECURITY CLASSIFICATION OF: a. REPORT Unclassified		17. LIMITATION OF ABSTRACT UL	18. NUMBER OF PAGES 15	19a. NAME OF RESPONSIBLE PERSON Birol Kara
b. ABSTRACT Unclassified				19b. TELEPHONE NUMBER (Include area code) 228-688-5577
c. THIS PAGE Unclassified				

Advantages of fine resolution SSTs for small ocean basins: Evaluation in the Black Sea

A. B. Kara,¹ C. N. Barron,¹ A. J. Wallcraft,¹ T. Oguz,² and K. S. Casey³

Received 27 September 2007; revised 21 February 2008; accepted 3 March 2008; published 7 August 2008.

[1] This paper examines monthly variability of climatological mean sea surface temperature (SST) in the Black Sea. A total of eight products, including observation- and model-based SST climatologies, are formed and compared with each other. Some of the observation-based SST data sets include only satellite measurements, while others combine in situ temperatures, such as those from moored and drifter buoys, with satellite data. Climatologies for numerical weather prediction (NWP) model-based data sets are formed using high temporal resolution (6 hourly) surface temperatures. Spatial resolution of these SST products varies greatly (\approx 4 km to 280 km), with the observation-based climatologies typically finer than the NWP-based climatologies. In the interior, all data sets are in general agreement, with annual mean SST biases typically within $\pm 0.2^{\circ}\text{C}$ in comparison to the finest resolution (4 km) satellite-based Pathfinder climatology. Major differences are near the land-sea boundaries where model-based SSTs pose serious biases (as much as $>5^{\circ}\text{C}$). Such errors are due to improper contamination of surface temperatures over land since coarse resolution model-based products cannot distinguish land and sea near the coastal boundaries. A creeping sea-fill interpolation improves accuracy of coastal SSTs from NWP climatologies, such as European Centre for Medium-Range Weather Forecast. All climatologies are also evaluated against historical in situ SSTs during 1942–2007. These comparisons confirm the relatively better accuracy of the observation-based climatologies.

Citation: Kara, A. B., C. N. Barron, A. J. Wallcraft, T. Oguz, and K. S. Casey (2008), Advantages of fine resolution SSTs for small ocean basins: Evaluation in the Black Sea, *J. Geophys. Res.*, 113, C08013, doi:10.1029/2007JC004569.

1. Introduction

[2] The ocean is one of the key elements in the climate system through transports of heat and fresh water and exchanges of these with the atmosphere. Sea surface temperature (SST) plays an important role in these exchange processes, especially through sensible heat flux, in heating or cooling the ocean [e.g., Fairall *et al.*, 2003]. In turn, surface heat fluxes may provide a negative feedback process for SST under some circumstances. Having reliable information about climatological mean SST is therefore essential for understanding these larger balances.

[3] Obtaining accurate SST fields is even a more challenging task for semi-enclosed or enclosed basins, such as the Black Sea, because such relatively small basins are dominated by coastline orientation, shape and topography, making the spatial resolution of a given data set an important factor. In particular, the Black Sea is an ideal

basin for examining SST variability in order to explore the importance of spatial resolution due to the existence of a wide continental shelf. Changes in SST have also been shown to have strong influence on the biological properties of the region [e.g., Oguz *et al.*, 2003]. For example, a SST product having a spatial resolution of 4 km, as shown in Figure 1, could be quite different from one having much coarser spatial resolution, especially near the land-sea boundaries. A typical product from Numerical Weather Prediction (NWP) centers provides high temporal resolution (e.g., 6 h) historical surface temperatures over land and sea. However, as will be further discussed in section 2, their grid resolutions (e.g., $1.875^{\circ} \times 1.875^{\circ}$), are too coarse for the Black Sea, where the latitudinal range of the region is generally $<4^{\circ}$ and even less from east to west. Such NWP products do not have a clear distinction between land and sea at the coastline. Therefore they may not provide accurate information for a range of climate, biological and other studies, that rely on accurate SST products in the Black Sea.

[4] The need for a fine spatial resolution product is not the only reason that makes SST accuracy a challenging task in the Black Sea. Scattered in situ SST observations from moored buoys, conventional ship-based measurements, drifting buoys, etc., may not provide enough spatial and temporal coverage to construct a reliable climatology. While frequent repeat observations and coverage of satel-

¹Naval Research Laboratory, Oceanography Division, Stennis Space Center, Mississippi, USA.

²Institute of Marine Sciences, Middle East Technical University, Erdemli, Icel, Turkey.

³NOAA National Oceanographic Data Center, Silver Spring, Maryland, USA.

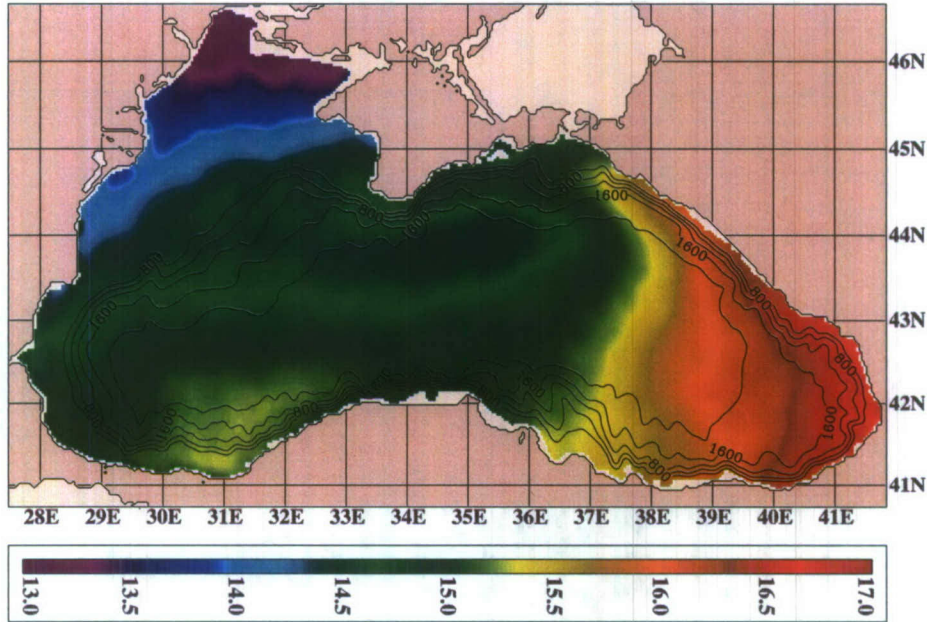


Figure 1. Climatological (annual) mean SST ($^{\circ}$ C) in the Black Sea. Bottom topography contours are also overlain, starting from 400 m with 400 m intervals.

lite-based SST measurements can be sufficient for creating a fine resolution gridded SST product, they may suffer from excessive cloudiness over the Black Sea, which is typically influenced by European or Siberian air masses and various teleconnection patterns [e.g., *Oguz et al.*, 2006]. Because most of these satellite systems have relied on infrared estimates, clouds would limit accuracy of spatially varying SST fields [e.g., *Kara and Barron*, 2007].

[5] No systematic analyses and assessment of SST variability provided by different data sources are available in the Black Sea. The present paper serves this purpose and provides a comprehensive analysis of SST variability in the Black Sea, constructed by a total of eight observation- and NWP model-based products. In particular, major purposes of this paper are to (1) introduce and examine SST climatologies from a variety of sources, (2) discuss their accuracies with respect to a fine resolution satellite-based data set and in situ data, (3) demonstrate possible inaccuracies in NWP SSTs resulting from land contamination near the coastal boundaries due to coarse grid resolution, and (4) propose a creeping sea-fill methodology to reduce land contamination in forming SST climatologies.

2. SST Products

[6] Table 1 lists the product abbreviations used throughout the text. All climatologies are configured for the global ocean, and their grid resolutions are given in Table 2, along with the original sampling time periods and data sources used for constructing them. For the purpose of this study, monthly mean SST from each climatology is processed for the Black Sea as will be described in section 2.2. There are other sources of SST climatologies which can be directly

obtained or formed from their data, but in this paper we limit ourselves readily available global ones.

2.1. Description of SST Climatologies

[7] The first product in Table 1 is the satellite-based 4 km resolution PATHF climatology. The original version of Pathfinder SST climatology (version 4) is at \approx 9 km resolution [*Kilpatrick et al.*, 2001]. It is derived from Advanced Very-High Resolution Radiometer (AVHRR) Pathfinder SST data during 1985–2001. The data processing was done using Infrared observations from National Oceanic and Atmospheric Administration (NOAA) polar orbiting satellites. The major shortcoming of this data set is the relatively crude land-mask, creating significant problems for coastal applications. Later, another version of the climatology was released. The updated product uses most of the same techniques presented by *Casey and Cornillon* [1999], and

Table 1. Data Sources From Which Monthly SST Climatologies Were Obtained or Formed^a

Acronym	Name of the SST Product
PATHF	Advanced Very High Resolution Radiometer (AVHRR) Pathfinder
MODAS	Modular Ocean Data Assimilation System
NOAA	National Oceanic and Atmospheric Administration
WOA01	World Ocean Atlas 2001
NOGAPS	Navy Operational Global Atmospheric Prediction System
ERA40	European Centre for Medium-Range Weather Forecasts
NCEP1	National Centers for Environmental Prediction, Re-Analysis 1
NCEP2	National Centers for Environmental Prediction, Re-Analysis 2

^aTime period during which SST climatology was formed is different for each product.

Table 2. Time Intervals and Grid Resolutions for SST Products

Data Set	Interval	Grid Resolution	Time	Reference	Data Source
PATHF	1985–2001	$0.040^\circ \times 0.040^\circ$	variable	Casey and Cornillon [1999]	satellite
MODAS	1993–2005	$0.125^\circ \times 0.125^\circ$	daily	Barron and Kara [2006]	satellite only
NOAA	1971–2000	$1.000^\circ \times 1.000^\circ$	variable	Reynolds et al. [2002]	satellite, in situ
WOA01	1773–2001	$1.000^\circ \times 1.000^\circ$	variable	Stephens et al. [2002]	in situ only
NOGAPS	1998–2005	$1.000^\circ \times 1.000^\circ$	3 hourly	Rosmond et al. [2002]	model-based
ERA40	1979–2002	$1.125^\circ \times 1.125^\circ$	6 hourly	Källberg et al. [2004]	model-based
NCEP1	1979–2002	$1.875^\circ \times 1.875^\circ$	6 hourly	Kalnay et al. [1996]	model-based
NCEP2	1979–2002	$1.875^\circ \times 1.875^\circ$	6 hourly	Kanamitsu et al. [2002]	model-based

has a resolution of 4 km. Key improvements in the new PATHF climatology include a more accurate, consistent land mask. The monthly climatologies were derived using data only with a quality flag of 7. A median filter is applied to fill in the data gaps, and a median smoother is used for the entire field to remove small-scale noise. Note that a new Pathfinder climatology using 1985–2006 is actively being developed at NOAA, and it is not available as of this writing.

[8] Unlike PATHF, the NOAA SST climatology was constructed using both in situ and satellite SSTs for the 1971–2000 base period as described by Reynolds et al. [2002]. In situ data are obtained from ships and buoys, including both moored and drifting buoys. These are combined with SSTs from AVHRR satellite retrievals to obtain the final product. NOAA SST is provided on a $1^\circ \times 1^\circ$ grid over the global ocean. The climatology was built from two intermediate climatologies: a 2° SST climatology developed from in situ data for the period 1971–2000, and a 1° SST climatology for the period 1982–2000 derived from the second version optimum interpolation (OI) SST analysis. In the midlatitudes, including the Black Sea, the changes in NOAA SST are largely due to the difference in the base period and are typically small, with absolute differences generally $<0.2^\circ\text{C}$.

[9] MODAS SST is a purely satellite-based product [Barron and Kara, 2006], covering 1993–2005. It is produced on a uniform $1/8^\circ$ (latitude, longitude) grid by an OI of AVHRR nonlinear SST observations processed by the Naval Oceanographic Office [May et al., 1998]. All operational global AVHRR data from 1993 to the present have been used in the MODAS analysis, reflecting on any given day the collected global coverage data from one to three of the NOAA polar orbiters. The OI approach is based on joint emphasis of both SST accuracy and fidelity in locating and quantifying SST gradients. The MODAS analysis uses a Gaussian error covariance with 60-h time and 20-km length scales, smaller than those used in the NOAA climatology. These scales were determined subjectively to balance fidelity in representing fronts with mitigation of spurious gradients around data-sparse regions. For extended cloudy periods, the first guess and its expected error tend toward climatological means and standard deviations.

[10] The WOA01 climatology does not include any satellite-based measurements. It is based on observational SSTs from various sources, such as drifting buoy data and expendable bathythermograph (XBT) measurements. The time period (1773–2001) during which the climatology constructed is the longest one in comparison to other

products (Table 2). SSTs used in WOA01 were averaged by 1° squares for input to the objective analysis [e.g., Thiebaux and Pedder, 1987; Daley, 1991]. The initial objective analyses usually contained some large-scale gradients over a small area, or bulls eyes. These unrealistic features generally occurred because of the difficulty in identifying nonrepresentative values in data sparse areas.

[11] Of the monthly SST climatologies formed from 6 hourly SSTs from NWP centers, NOGAPS is the finest resolution ($1^\circ \times 1^\circ$) of all the model products (Table 2). As in other NWP products, NOGAPS applies a modern variational data assimilation technique for the past conventional and satellite observations. The ERA-40 project obtained a comprehensive archive of past observations from the National Centers for Environmental Prediction (NCEP) to supplement its original observational archives. Two NCEP re-analysis products (NCEP1 and NCEP2) have relatively coarse grid resolutions of $1.875^\circ \times 1.875^\circ$. Obviously, such grid resolution is even too coarse for a small ocean basin, such as the Black Sea. NCEP2 is intended to improve NCEP1 by fixing the errors and by updating the parameterizations of the physical processes. Similar to the ERA-40 product, 6 hourly SSTs were used to form monthly SST climatologies from NCEP1 and NCEP2 during the common time period of 1979–2002. Further details about each NWP-based product, including model parameterizations and data assimilation procedures, can be found in the references provided in Table 2.

2.2. Construction of SST Climatologies for the Black Sea

[12] We obtain monthly SST climatologies for PATHF, NOAA and WOA01 directly from their original sources. These are termed observation-based products since they are based on various type of observational SSTs (e.g., buoy, XBT, CTD) and satellite measurements of SST. Observational sampling is highly variable, and these products use different interpolation techniques and smoothing procedures to form monthly mean SST fields. We produced an observation-based monthly SST climatology from equally weighted daily MODAS SST analyses from 1993 through 2005.

[13] We construct monthly SST climatologies from model outputs which are available from NWP centers. These so-called operational or re-analyzed model-based products are NOGAPS, ERA40, NCEP1 and NCEP2 and have high temporal resolution (6 h). NWP centers provide surface temperature values both over land and sea. They cannot distinguish a precise transition between land and sea due to their limited grid resolutions. The temperature on the water

surface is actually called SST, while surface temperature over land is typically designated as soil temperature.

[14] ERA40, NCEP1, and NCEP2 have a common time period 1979–2002 during which monthly climatologies are formed using 6 hourly SST outputs at each ocean grid (Table 2). Climatologies were formed starting from 1979 since earlier time periods did not include sufficient observational data to constrain the assimilation. The common interval eliminates potential differences associated with the sampling period, and the 24-year length (1979 to 2002) is sufficient to produce a reasonable climatology. Unfortunately, NOGAPS data do not extend to years prior to 1998, limiting us to use 6 hourly SSTs starting from 1998. Thus for NOGAPS a 8-year climatology (1998–2005) is formed.

3. Main Features of SST Climatologies

[15] Monthly mean SST variability from all products described in section 2 is examined for the Black Sea. Throughout the text we follow *Locarnini et al.* [2006] in our definition of the Northern Hemisphere seasons: January, February, and March (winter); April, May, and June (spring); July, August, and September (summer); October, November, and December (fall). For consistency, SSTs from all products are interpolated to a common grid of 4 km, the finest resolution of the products considered (i.e., PATHF).

3.1. Monthly SST Variability in the Black Sea

[16] Climatological annual mean of SST formed from monthly mean PATHF is already shown to demonstrate overall SST variations in the entire basin (Figure 1). The climatology is from 4 km monthly mean PATH SST values, and formed from measurements from the NOAA polar orbiting satellites during 1985–2001. Each satellite was launched in a sun-synchronous orbit, with specified ascending and descending node times. The ascending node time is the time when the satellite passes from south to north over the equator, and the descending node time is when it passes from north to south over the equator. Each orbit requires about 102 min to complete, and the swaths observed by the satellite overlap, resulting in possibly multiple observations from multiple orbits at any given spot on Earth. The Pathfinder algorithm combines the multiple observations as long as they have the same quality level.

[17] The bottom topography for the Black Sea in Figure 1 was constructed from the 1 minute resolution data from General Bathymetric Chart of the Oceans (GEBCO) available online at <http://www.bodc.ac.uk/products/bodc-products/gebco/>. The northwestern shelf where the water depth is typically <100 m is the coldest region, with SST values generally <14.5°C. The easternmost part of the Black Sea is the warmest, with mean SST exceeding >16°C. The most interesting feature of the annual mean SST map is the existence of fronts over the northwestern shelf (colors in blue and cyan) and the eastern region (yellow), evident from relatively fine resolution PATHF climatology, revealing the importance of horizontal resolution in identifying such features in a small ocean basin, such as the Black Sea.

[18] Here, for simplicity, we show SSTs in February, May, August, and November (i.e., midmonths of each season) to represent winter, spring, summer and fall, re-

spectively (Figure 2). Spatial variability in monthly SST from all products clearly reveals commonly known relatively warm SSTs in the easternmost part of the Black Sea and cold SSTs in the northwestern shelf. SSTs from the fine resolution PATHF and MODAS reveal existence of distinct ocean fronts in the northwestern shelf in February and partly in November. These are less evident in other products and during other time periods. All SST climatologies (except NCEP2) exhibit relatively warm temperatures in the easternmost part of the Black Sea in all months with respect to the rest of the region.

[19] The most notable feature of spatial SST evident from Figure 2 is the existence of unrealistically low SSTs near the land-sea boundaries. Such features are noted from all NWP products (NOGAPS, ERA40, NCEP1 and NCEP2), and they are highly questionable in comparison to the observation-based climatologies. The problem is particularly serious for NCEP1 and NCEP2, both of which are the coarsest resolution ($1.875^\circ \times 1.875^\circ$) NWP products. The main reason for these unrealistic values is that some of the ocean points near the coastal boundaries are contaminated by land values. This means that terrestrial surface soil temperature from NWP products becomes mapped over the sea, affecting SST because the grid point cannot separate land or sea. Because NCEP has relatively coarse resolution, the land contamination is significantly large. Knowing that the land-sea heterogeneity, such as the land roughness length that affects heat transfer can be significantly larger than ocean and makes surface temperature just above the land typically different than temperature on the sea surface. Further details about the reasons of incorrect SST from NWP products near land-sea boundaries will be discussed in section 4.

[20] Basin-averaged SST is calculated in the Black Sea, providing a summary of monthly means for each product (Figure 3). A strong seasonal cycle in SST is evident from all products. Roughly, a basin-averaged mean SST value of 8°C during winter increases by 15°C, to a value of $\approx 22^\circ\text{C}$ during summer. This is generally evident from all SST climatologies (Figure 3a). MODAS appears to have the warmest SSTs, while NCEP1 and NCEP2 are cool outliers, having relatively colder SSTs in all months (Table 3). Land contamination of surface temperature to SST near coastal boundaries is main reason of such cold temperatures as will be described in detail.

[21] Taking the finest resolution PATHF climatology as a reference, monthly mean differences in basin-averages SSTs are computed. While observation-based MODAS, NOAA and WOA01 climatologies are generally slightly warmer ($<0.5^\circ\text{C}$) than PATHF, NWP model-based climatologies are often significantly colder ($>0.5^\circ\text{C}$) than PATHF climatology (Figure 3b). A separate study is underway to clearly identify why the PATH and NOAA climatologies are biased with respect to each other, but possible reasons include differing cloud masking techniques and approaches to account for water vapor contamination of the infrared measurements from the AVHRR instruments.

[22] Unlike the other observation-based climatologies, MODAS has consistent warm bias in all months. This warm bias is due mostly to relaxation fields in the satellite-based MODAS SST analysis. MODAS includes no in situ obser-

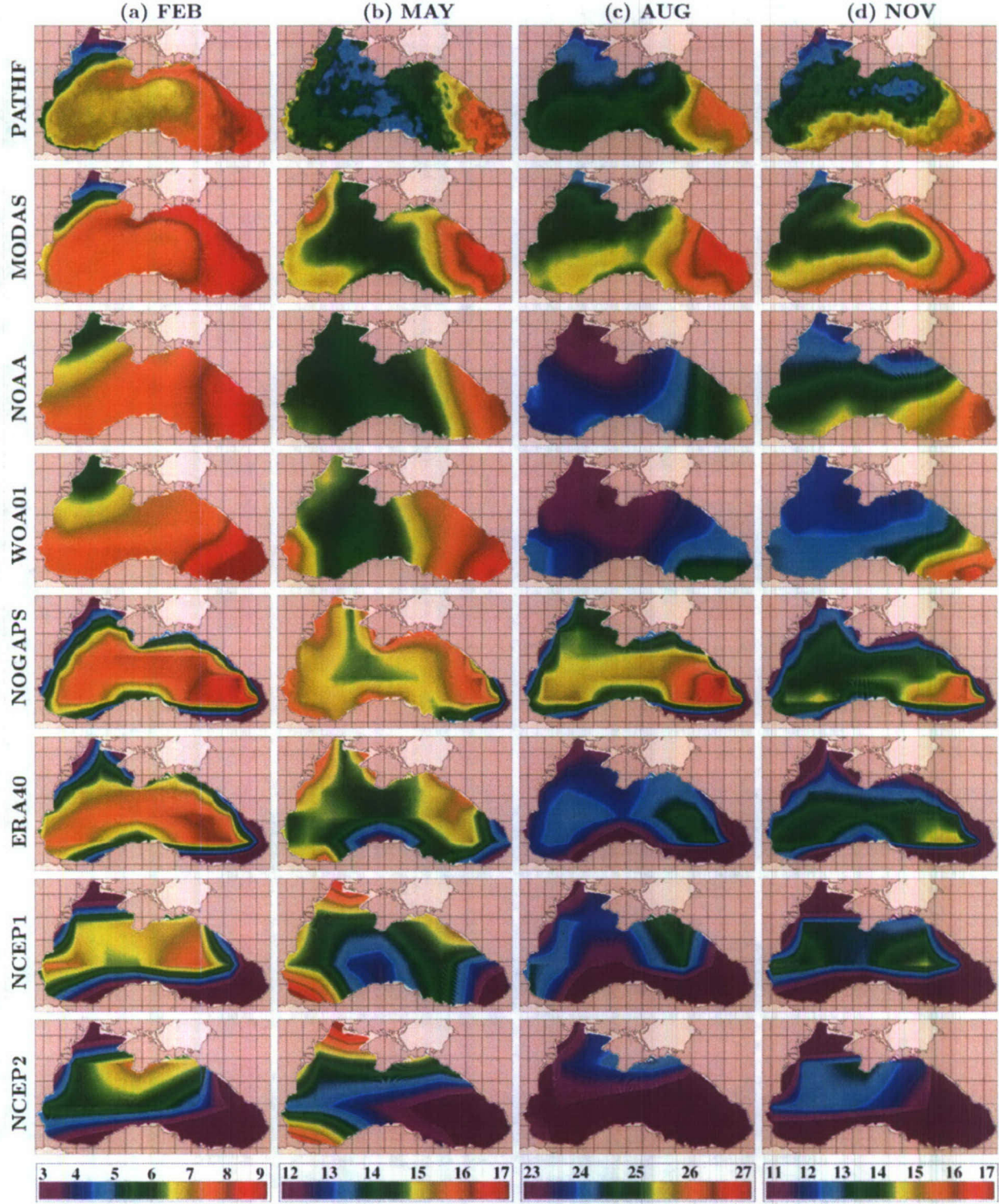


Figure 2. Climatological mean SST constructed from eight different data sources in February, May, August, and November. Abbreviations for each data source are provided in Table 1.

vations so background relaxation becomes important during persistently cloudy periods, such as the Black Sea winter. That is typically the main source of the MODAS SST bias [Kara and Barron, 2007].

3.2. Evaluations of SST Climatologies

[23] For statistical comparisons of SST climatologies, monthly mean values from each product are used. The finest resolution (4 km) PATHF is taken as the standard

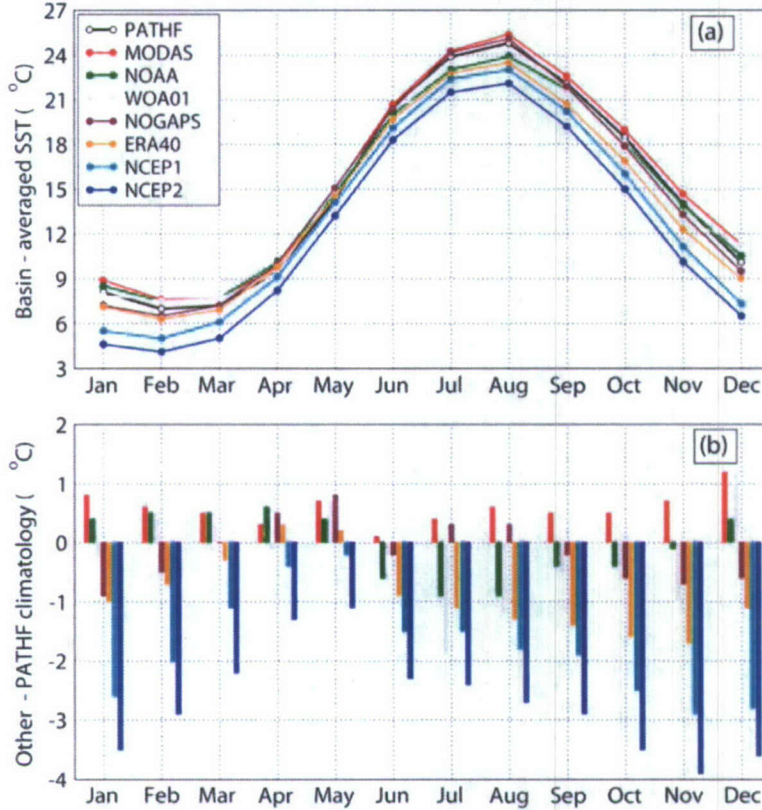


Figure 3. (a) Basin-averaged monthly mean SST averaged in the Black Sea, and (b) the basin-averaged monthly mean SST difference for each climatology when SST from Pathfinder is subtracted from the corresponding monthly SST from other climatologies.

SST product, i.e., other products are evaluated with respect to the PATHF climatology. Monthly mean time series of SST at each ocean grid point from PATHF and others are compared using two statistical metrics: mean error (ME), root mean square (RMS) difference.

[24] Let X_i ($i = 1, 2, \dots, 12$) be the set of 12 monthly mean PATHF SST values, and let Y_i ($i = 1, 2, \dots, 12$) be the set of 12 monthly mean “other” SST values, where the other refers to each of MODAS, NOAA, WOA01, NOGAPS, ERA40, NCEP1, and NCEP2. In addition, let \bar{X} (\bar{Y}) and σ_X (σ_Y) be the means and standard deviations of the PATHF

(other) values, respectively. ME and RMS are then expressed as follows:

$$ME = \bar{Y} - \bar{X}, \quad (1)$$

$$RMS = \left[\frac{1}{n} \sum_{i=1}^n (Y_i - X_i)^2 \right]^{1/2}, \quad (2)$$

Here, ME simply represents annual mean bias of SST products with respect to the PATHF climatology, and RMS

Table 3. Basin-Averaged Monthly Mean SST in the Black Sea

Month	PATHF, °C	MODAS, °C	NOAA, °C	WOA01, °C	NOGAPS, °C	ERA40, °C	NCEP1, °C	NCEP2, °C
Jan	8.1	8.9	8.5	7.9	7.2	7.1	5.5	4.6
Feb	7	7.6	7.5	7.5	6.5	6.3	5	4.1
Mar	7.2	7.7	7.7	7.7	7.2	6.9	6.1	5
Apr	9.5	9.8	10.1	9.4	10	9.8	9.1	8.2
May	14.3	15.0	14.7	15	15.1	14.5	14.1	13.2
Jun	20.6	20.7	20	20.4	20.4	19.7	19.1	18.3
Jul	23.9	24.3	23	22	24.2	22.8	22.4	21.5
Aug	24.8	25.4	23.9	23.6	25.1	23.5	23	22.1
Sep	22.1	22.6	21.6	21.6	21.9	20.7	20.2	19.2
Oct	18.5	19	18.1	18.1	17.9	16.9	16	15
Nov	14	14.7	13.9	13	13.3	12.3	11.1	10.1
Dec	10.1	11.3	10.5	11.3	9.5	9	7.3	6.5
Mean	15	15.6	14.9	14.8	14.9	14.1	13.2	12.3

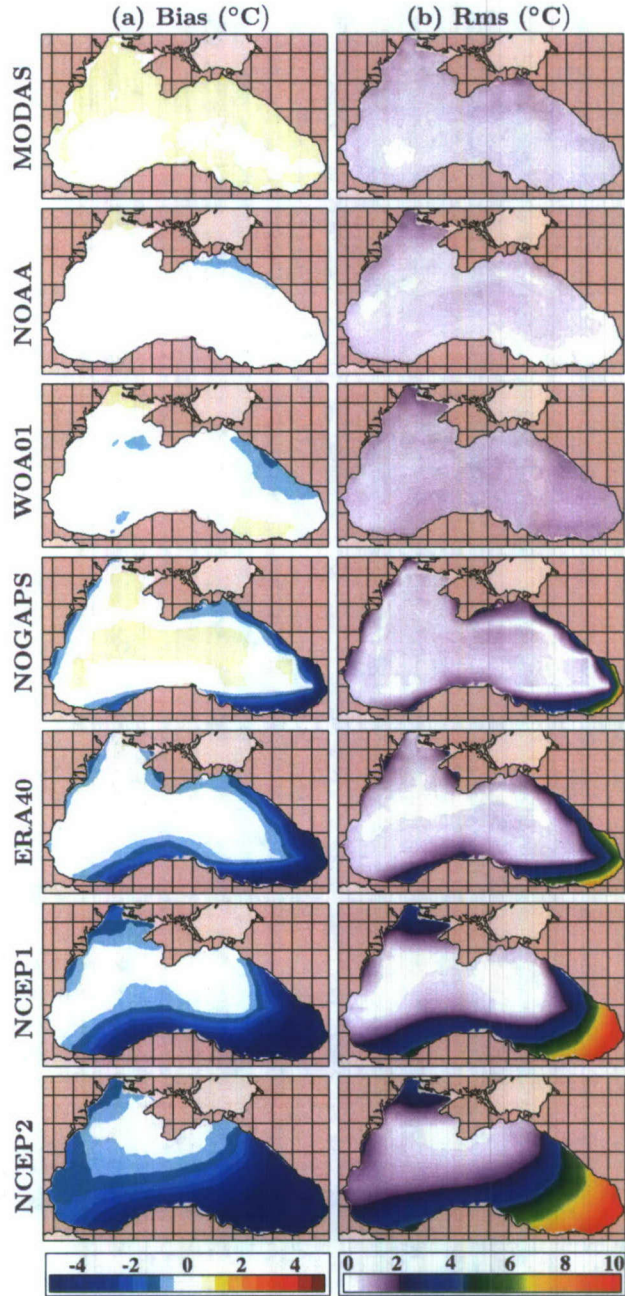


Figure 4. Spatial maps of annual mean bias (ME) and RMS difference between Pathfinder SST climatology and other ones. For ME, the Pathfinder SST is subtracted from other climatologies, and RMS SST difference is calculated over the seasonal cycle as explained in the text.

is absolute measure of the distance between the SST time series. RMS difference is calculated over the seasonal cycle.

[25] Spatial maps of mean SST bias and RMS SST difference calculated at each ocean grid based on monthly mean values are shown in Figure 4. All products agree well in the interior of the Black Sea. Annual mean SST bias with respect to the PATHF climatology is within $\pm 0.5^{\circ}\text{C}$ (Figure 4a). The agreement is remarkable even though the periods during which the observation-based SST climatologies were formed are different (Table 2). Even SSTs from

NWP model-based products of NOGAPS, ERA40, NCEP1, and NCEP2 are very similar to those from PATHF in the interior where there is no land-contamination of surface temperature.

[26] RMS SST differences are generally small ($<1^{\circ}\text{C}$) in the interior except for the coarse resolution NCEP products, both of which have relatively large RMS SST differences with respect to PATHF, especially in the eastern part of the region (Figure 4b). In fact, basin-averaged RMS values are the largest with values of 2.2°C and 3°C for

Table 4. Basin-Averaged SST Error Statistics in the Black Sea

Product Comparison	ME, °C	Rms, °C
PATHF versus MODAS	0.4	0.7
PATHF versus NOAA	-0.1	0.6
PATHF versus WOA01	-0.2	0.9
PATHF versus NOGAPS	-0.1	1.1
PATHF versus ERA40	-0.9	1.3
PATHF versus NCEP1	-1.8	2.2
PATHF versus NCEP2	-2.7	3

NCEP1 and NCEP2 (Table 4). Note that both ME and RMS are computed at each grid point, and basin averages are then found. Although ME and RMS are typically large for NCEP1 and NCEP2 in comparison to other products, those are mostly from errors near the land-sea boundaries due to improper representation of land-sea masks (see section 4).

[27] Box-plots of annual mean SST bias and RMS SST difference shown in Figure 4 are produced to identify outliers and compare distributions for each SST product. The box for each product contains the middle 50% (i.e., median) of the annual mean bias (Figure 5a) and the RMS SST difference (Figure 5b). Median ME and RMS values are generally similar to each other for all products except for NCEP1 and NCEP2. The upper (lower) hinge of the box in the plots marks the 75th (25th) percentile of the ME and RMS. The range of the middle two quartiles is known as the interquartile range, which is very close to each other for the observation-based SST climatologies of MODAS, NOAA and WOA01. The median values within the box are not equidistant for the NWP model-based climatologies, revealing that both ME and RMS are skewed. As further evident from the lower whiskers in Figure 5, SSTs from NOGAPS, ERA40, NCEP1 and NCEP2 can be colder than PATHF by 8°C or even more. Similarly, RMS SST differences with respect to PATHF can even be as large as 10°C or more for NCEP1 and NCEP2.

[28] Finally, we further examine SST differences among the observation-based climatologies, given that they provide similar SSTs in comparison to these from PATHF. For this purpose, plots for mean SST bias and RMS SST difference for MODAS, NOAA, and WOA01, which are already shown in Figure 4, are reproduced but with much smaller intervals (Figure 6). The most impressive feature is that there is almost no mean SST bias between PATHF and NOAA. In fact, NOAA SST bias in comparison to PATHF are within $\pm 0.2^\circ\text{C}$ for 81.2% of the Black Sea. Note that we do take into account weights by actual grid cell area in computing percentage values (Figures 6a and 6b). Not surprisingly, SSTs in the NOAA SST climatology is created using a bias adjustment procedure. As explained by *Smith and Reynolds* [1998], while the seasonal cycle of the adjustment has an amplitude of $\leq 0.3^\circ\text{C}$ at most inland seas over the global ocean, the amplitude exceeds 0.5°C in the relatively small Black Sea. The MODAS SST is systematically warmer than the PATHF SST, with 47.8% of the bias values are $\geq 0.2^\circ\text{C}$ but $< 0.4^\circ\text{C}$. The analysis presented in the next subsection suggests that this can mainly be due to sampling bias, with warmer conditions on average during 2002–2005 than the PATHF period of 1985–2001. How-

ever, RMS SSTs for MODAS and NOAA are generally similar (Figures 6c and 6d).

3.3. Sampling Period for SST Climatologies

[29] There can be many factors contributing differences among the SST products. Of the NWP model-based SST climatologies of NOGAPS, ERA40, NCEP1 and NCEP2, the last three were all formed during 1979–2002 as mentioned earlier. This rules out the possibility of differences resulting from the time period. Possible reasons for differences among these products are that numerical models from the NWP centers have different boundary layer parameterizations, data assimilation methods and different types of satellite SSTs used in the assimilations. Therefore differences in SSTs do exist regardless of the fact that climatologies from last three were formed using the same time interval of 1979–2002.

[30] In addition to the above mentioned factors, systematic errors of the assimilation model clearly influence analyses in data-sparse regions such as the Black Sea, while the strength of operational products is that they provide gridded data with high temporal resolution (i.e., 6 hourly). NCEP2 re-analysis was initially performed to fill the shortcomings of NCEP1 re-analysis. However, we demonstrated that SSTs from NCEP2 are slightly worse than those from NCEP1. The reasons of why the SST from the second re-analysis turned out to be worse than the first one are beyond the scope of this paper.

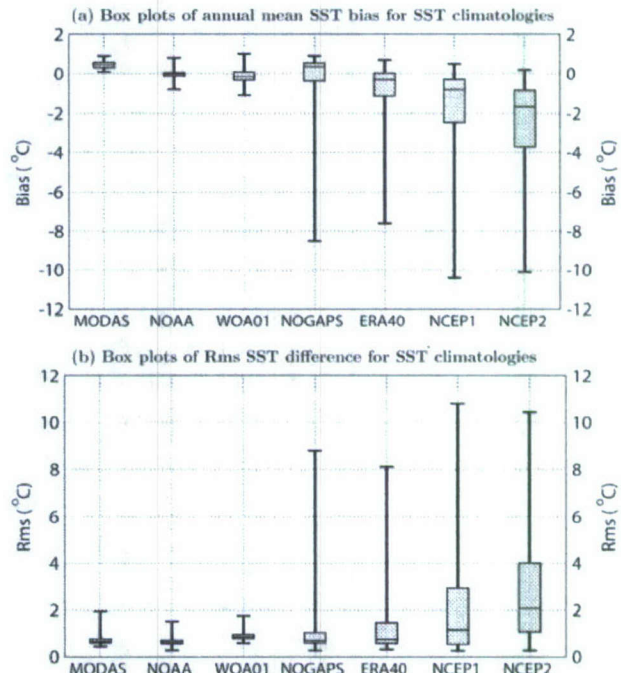


Figure 5. Box-plots of (a) annual mean SST bias and (b) RMS SST difference over the seasonal cycle. Both are with respect to the Pathfinder climatology. The box plot for each SST product shows median (drawn as a line in the box), lower (25%) and upper quartiles (75%). The ends of the vertical lines (i.e., whiskers) indicate the minimum and maximum bias or RMS values in the Black Sea.

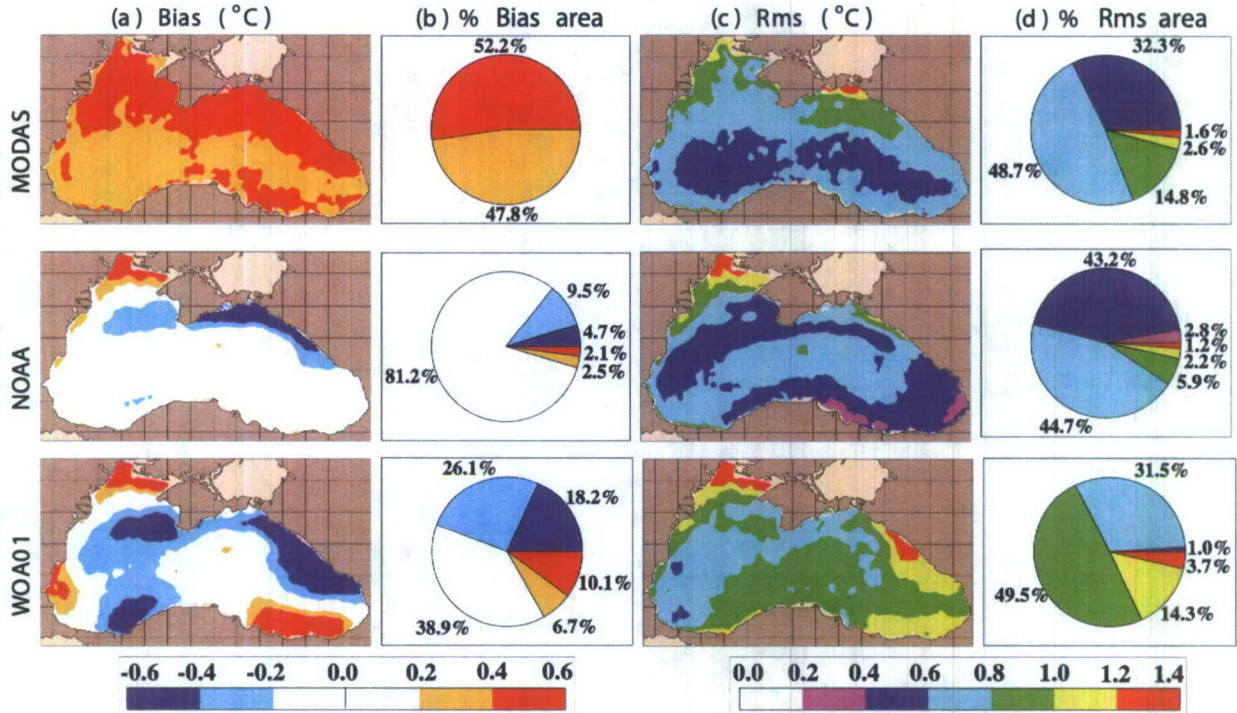


Figure 6. Statistical evaluation of MODAS, NOAA, and WOA01 climatologies in comparison to the Pathfinder climatology: (a) Annual mean SST bias, (b) percentage of the region covered by bias values, (c) RMS SST difference, and (d) percentage of the region covered by RMS differences.

[31] What accounts for the differences among the observation-based climatologies, particularly the higher-resolution Pathfinder and MODAS? Significant differences may arise between the climatologies if SST data are not stationary over the time periods sampled. In typical construction of climatologies, SSTs are assumed to be stationary, meaning that the mean, variance and autocorrelation of the data are constant over time [e.g., *Bendat and Piersol, 2000*]. If SST data are stationary, then climatologies formed using different and sufficiently large samples are expected to produce a common mean. If the data are not stationary, temporal differences in sampling are likely to produce skewed statistics. For example, we recognize that the seasonal variation in SST introduces a nonstationary component. If a sample results in significantly more summer observations than winter, we would likely produce a warm bias in our estimate of the mean. The impact of the nonstationary seasonal variation can be mitigated by binning the data by seasons or months, calculating the statistics over these time bins, and determining multi-annual mean statistics using equally weighted bin statistics. We assume that the seasonal sampling has been appropriately balanced in the construction of the climatologies examined in this study.

[32] Here, we investigate whether the biases between the MODAS and Pathfinder means may be due to skewed sampling in the presence of a multi-annual warming trend, a trend that introduces a nonstationary component into the SST time series. The SST data contributing to the Pathfinder and MODAS climatologies cover different time periods (Table 2). Assuming data contributing to each

climatology are evenly distributed over each sampling interval, the mean sample dates for Pathfinder and MODAS are mid-1993 and mid-1999, giving a difference of 6 years. The warming trend over the MODAS sampling interval is shown in Figure 7. The slope of the 1993–2005 linear fit is $\approx 0.003^{\circ}\text{C}/\text{month}$. If we extrapolate this trend over the Pathfinder sampling period, the expected difference Pathfinder and MODAS SST means would equal the SST trend slope multiplied by the difference between the mean sample dates, $\approx 0.2^{\circ}\text{C}$ (i.e., 6 years $\times 0.003^{\circ}\text{C}/\text{month}$). If instead the slope determined over 1993–2001 ($\approx 0.008^{\circ}\text{C}/\text{month}$) were extrapolated over the Pathfinder interval, the warm bias of MODAS climatology relative to Pathfinder would be even larger, close to $\approx 0.4^{\circ}\text{C}$. The magnitude of the bias introduced by sampling accounts for much of the MODAS warm bias in Figure 6.

[33] These results are consistent with *Oguz et al. [2006]*, which uses Black Sea winter SST to identify a cold phase from 1980–1994 followed by a neutral period from 1995–1998 and a warm phase beginning 1999. Thus, Pathfinder included relatively few warm phase measurements, while MODAS incorporated relatively few cold phase samples. We estimate from the original Figure 1a of *Oguz et al. [2006]* that a warm or cool phase differs by $\approx 0.25^{\circ}\text{C}$ from the neutral phase. About 10 years of the Pathfinder observations and 2 years of the MODAS observations are from the cold phase, while about 3 years of the Pathfinder and 7 years of the MODAS samples are from the warm phase. The implied temperature difference MODAS-PATHF is

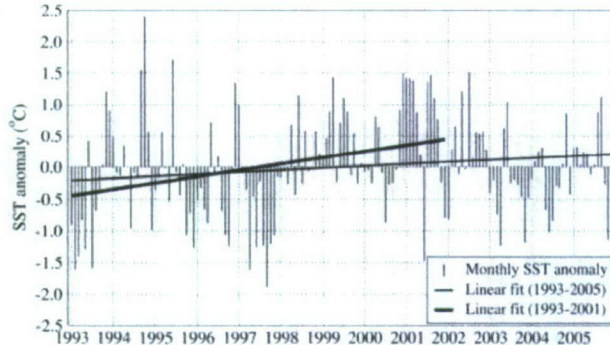


Figure 7. Monthly SST anomalies from MODAS from 1993 through 2005. Each daily MODAS SST is produced by a similar OI of AVHRR observations. Production of SST anomalies using a combination of OI and climatologically corrected persistence balances daily temporal resolution with improved transitions in time and space across cloud-obscured regions to eliminate data voids. The least squares lines are also shown for the time period of 1993–2005 and 1993–2001.

$-0.25^{\circ}\text{C} \times [(2/13)-(10/17)] + 0.25^{\circ}\text{C} \times [(7/13)-(3/17)]$, corresponding to a value of $\approx 0.2^{\circ}\text{C}$.

4. SST Accuracy Near the Coastal Regions

[34] In the preceding section, we mentioned that SSTs from NWP products are not accurate near the land-sea boundaries. As shown in Figure 4, they are too low in comparison to PATHF SST climatology. We asserted that such incorrect values are due to the land contamination of near-surface temperatures over land areas. Because NWP products provide gridded values, there is no discrimination between land and sea, causing misrepresentation of temperature over the sea. The focus of this section is to further elaborate on the reasons behind such errors.

4.1. Land Contamination of Surface Air Temperature on SST

[35] Incorrect SST values from NWP products near the coastal regions can mainly be attributed to improper representation of land-sea masks. The ocean and land areas in NOGAPS, ERA40, NCEP1, and NCEP2 are defined by a land-sea mask. The mask determines whether a particular grid point is land or sea. If the total fraction of a grid cell that is land exceeds 50%, then the grid point is classified as a land point; otherwise it is classified as a sea point. The land-sea masks in NOGAPS, NCEP1, and NCEP2 products are represented as values 0 (for sea) and 1 (for land). In the case of ERA40, the mask has values between 0 and 1, showing the fraction of land in that grid cell. Thus a value of 0.1 indicates that this point (cell) is 10% land and 90% ocean, and the ERA-40 actually calculates two different values for such grid points. To be consistent with other NWP products, we need a mask of zeroes and ones. Thus we picked 0.5 as the cut-off value for our land-masking of ERA40.

[36] Land-sea mask fields from each NWP center are first obtained at their original grids. They are then interpolated to a finer resolution (≈ 4 km) PATHF grid to demonstrate the

extent of land contamination over sea points (Figure 8a). For example, a contour value of 0.8 in the land-sea mask implies that a SST value is 80% contaminated by land values (i.e., near-surface temperature) over the ocean grid point. Land contamination over the ocean can be as much as 100% just near the boundaries. The contamination from land decreases systematically as one proceeds farther way from the coast to interior of the ocean. There is no land contamination in the regions covered in blue, mainly located in the interior of the Black Sea. Regions in red represent land. For PATH, all values are over the sea, thus there is no land contamination.

[37] Surface temperatures (i.e., soil temperature over land and SST over sea) from all NWP-products are shown in February (Figure 8b) and in May (Figure 8c). The values from PATHF solely represent SST over the sea, and taken as truth. It is obvious that temperatures over land are typically much colder than those over the sea. For example, climatological mean of PATHF SST is $>6^{\circ}\text{C}$ in the easternmost part of the Black Sea in February, and NWP products give surface temperatures of colder than -2°C just outside the eastern coast. Fluctuations on land temperatures are more than those on SST because the Black Sea is situated deep within the Eurasian landmass. The cold surface temperatures over land contaminate SST during the interpolation to the sea grid, resulting in the NWP products that indicate SSTs much lower than those from PATHF. This is even more problematic for NCEP1 and NCEP2 products due to their relatively coarse grid resolutions (Table 2). The same problem is less severe for the relatively finer NOGAPS, resulting in more accurate SSTs near the land-sea boundaries.

[38] Given the inaccurate representation of surface temperature near the coastal boundaries as mentioned above, one question to ask is “how large are SST errors from the NWP-based SST products in comparison to the PATHF climatology, depending on the extent of their land-sea masks?” We answer this question by repeating the statistical analysis presented in section 3 within and outside the land-sea masks. In other words, annual mean SST bias and RMS SST difference over the seasonal cycle are calculated for two regions: where the land-sea mask for the given NWP product has a value of only 0, and regions where the land-sea mask has a value >0 (Figure 8a). The former represents regions where there is no contamination from land values in SST, and the latter cover regions where the contamination varies from $>0\%$ to 100%.

[39] Mean SST bias and RMS SST difference with respect to PATHF is very small when calculated outside the extent of the land-sea mask (Table 5). Thus the NWP model-based SST products agree with the PATHF SST climatology in the interior quite well. Such agreement is even true for the coarse resolution NCEP1 and NCEP2, with RMS values of only 0.5°C and 1°C , respectively. When the same calculation is performed within the land-mask, those values increase dramatically, becoming 2.9°C and 3.8°C , resulting in 4.8 and 2.8 times increase in the RMS SST difference (Figure 9). The increase in the RMS for NCEP2 calculated within and outside the land-sea mask is not very large in comparison to that for NCEP1. The reason is that NCEP2 already has a larger SST bias with respect to PATHF outside the land-sea mask. Overall, statistical results presented here clearly reveal that all NWP-based SST

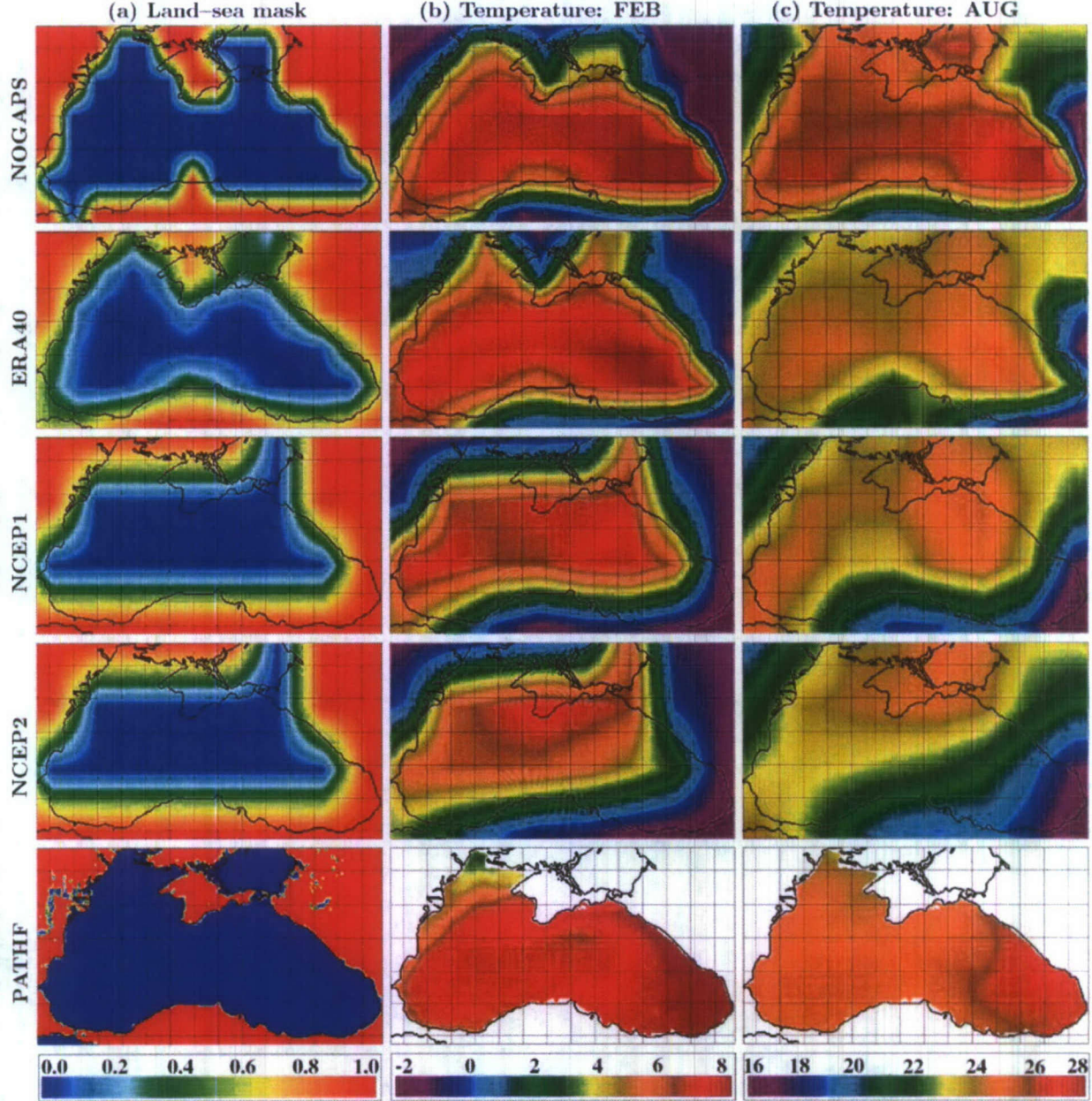


Figure 8. Land-sea masks (a) along with climatological mean surface temperatures in February (b), and August (b) in and around the Black Sea. Temperatures within the Black Sea coastline represent SST, while those outside the coastline are surface temperatures. Similar fields for the Pathfinder climatology are also included in the last row.

products do indeed agree with PATHF and other observation-based SST climatologies in the interior reasonably well.

4.2. Sea-Filled NWP SST Climatologies

[40] As demonstrated previously in Figure 8, SSTs from NWP products may have serious land contamination of near-surface air temperatures over the land. This could cause problems in forming accurate SST climatologies near the coastal boundaries. Here, we analyze whether such incorrect SSTs can be improved to have better agreement with observation-based climatologies.

[41] A solution for reducing improper representation of SST due to near-surface air temperatures over land near the coastal regions is to apply a creeping sea-fill methodology. Kara *et al.* [2007] gives details of the methodology. Simply, this technique uses SSTs which do not have any land contamination, i.e., only those SSTs inside the “blue” region of land-sea masks (see Figure 8a). These SSTs are then extrapolated into regions near the coast. Note that this process is applied at each 6 h time interval, and then a new climatology is formed in the same way as described in section 2.

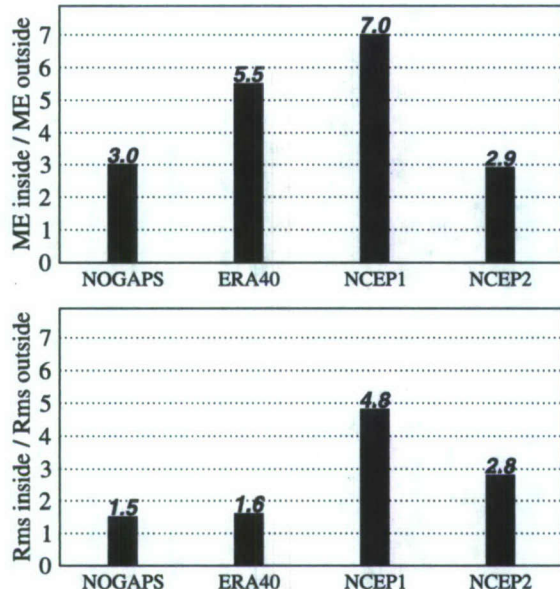


Figure 9. Increase in annual mean SST bias and RMS SST difference when they are calculated outside the land-sea mask versus within the land-sea mask. See also ME and RMS values in Table 5.

[42] As an example, SST climatologies resulting from the creeping sea-fill methodology are shown for all NWP products in February (Figure 10). The satellite-based PATHF is included as a truth since it does not have any contamination. After applying the creeping sea-fill, some of the land contamination is greatly reduced, especially for NOGAPS and ERA40. This can be seen from comparisons of SSTs in Figure 2a with Figure 10. Some of the major features of the spatial SST variability, e.g., fronts in the northwestern shelf, become better evident and more organized from the sea-filled NOGAPS and ERA40 climatologies. Unfortunately, even after applying the creeping sea-fill, NCEP1 cannot still represent realistic SST patterns in the northwestern shelf since its excessively coarse resolution does not allow proper extrapolation from SSTs in the interior. Similarly, large errors still exist in the sea-filled NCEP2 because SSTs in the interior are already too cold to extrapolate appropriate values to coastal regions. Here, it should be emphasized that while the sea-filled model-based climatologies are helpful, as in the Black Sea case, they could still be unable to recover specific and relevant structures inherent to a contrast, perhaps due to bottom topography or differences in thermal capacity between the ocean shelf and the adjacent continent.

5. Comparisons Against In Situ SSTs

[43] Following the climatology evaluation methods of [Casey and Cornillon, 1999], additional information on the relative performance of the individual climatologies is gained. These methods use in situ data as the standard of comparison and are based on the idea that the best-performing climatologies will minimize the standard deviation of the differences between those in situ data and the corresponding climatological values.

[44] We obtain observational SSTs from the International Comprehensive Ocean-Atmosphere Data Set (ICOADS), which provides the most extensive collection of surface marine data dating back to 1854 [Worley *et al.*, 2005]. ICOADS includes SSTs measured by various platforms, such as ship, drifting buoy, ocean station vessel etc., and we begin with all available SSTs during 1854–2007. A list including date of observation, latitude, longitude and in situ SST value was obtained from ICOADS, yielding an enormous amount of in situ SST (351,821 observations) at various points in the Black Sea. Observations prior to 1942 were excluded since they require significant bias corrections, leaving 266,298 in situ SST on which to base this analysis. At each point, we then extracted the corresponding climatological SST from each climatological SST product. For instance, for an in situ SST from ICOADS collected on 1 March 1980, we extract the March climatological value at that location from each climatology. After interpolating all of the climatologies to the PATH grid, we simply select the closest pixel to the in situ latitude/longitude location.

[45] The standard deviation and mean of these anomalies are then computed for each climatology and provided in Table 6. Relatively large standard deviations around the bias reflects the natural interannual variability of the SST in the Black Sea. Overall, the standard deviation around the biases for the observation-based SST products agree remarkably well with identical values of $\approx 2.3^{\circ}\text{C}$. On the contrary, NWP products give relatively high standard deviations compared to the very large number (266,298) of in situ observations (Table 6). For example, NCEP1 and NCEP2 have standard deviation of $>3^{\circ}\text{C}$, resulting in an increase of $\approx 30\%$. This analysis further confirms relatively large biases in the NWP-based SST climatologies as discussed in sections 3 and 4. Similar computations were also repeated outside the land-sea mask for NWP products, resulting in lower standard deviations of 2.33° , 2.39° , 2.47° , and 2.61°C for NOGAPS, ERA40, NCEP1, and NCEP2, respectively. Thus the land contamination of SST near the coastal boundaries is also evident from the evaluations with respect to in situ data.

[46] Many factors, such as the varying depths of ICOADS surface observations and the differing measurement tech-

Table 5. Same as Table 4 but Calculated Within and Outside the Land-Sea Mask

Product Comparison	Region	Mean, $^{\circ}\text{C}$	Min, $^{\circ}\text{C}$	Max, $^{\circ}\text{C}$
ME, $^{\circ}\text{C}$				
PATHF versus NOGAPS	Within	-0.8	-8.5	0.9
	Outside	0.4	-1.5	0.9
PATHF versus ERA40	Within	-0.9	-7.6	0.7
	Outside	0.2	0.0	0.3
PATHF versus NCEP1	Within	-2.4	-10.4	0.5
	Outside	-0.3	-1.1	0.2
PATHF versus NCEP2	Within	-3.5	-10.1	0.2
	Outside	-0.9	-3.4	0.2
Rms, $^{\circ}\text{C}$				
PATHF versus NOGAPS	Within	1.5	0.3	8.9
	Outside	0.6	0.3	2.2
PATHF versus ERA40	Within	1.3	0.3	8.1
	Outside	0.5	0.4	0.6
PATHF versus NCEP1	Within	2.9	0.3	10.9
	Outside	0.5	0.3	1.2
PATHF versus NCEP2	Within	3.8	0.3	10.4
	Outside	1	0.3	3.4

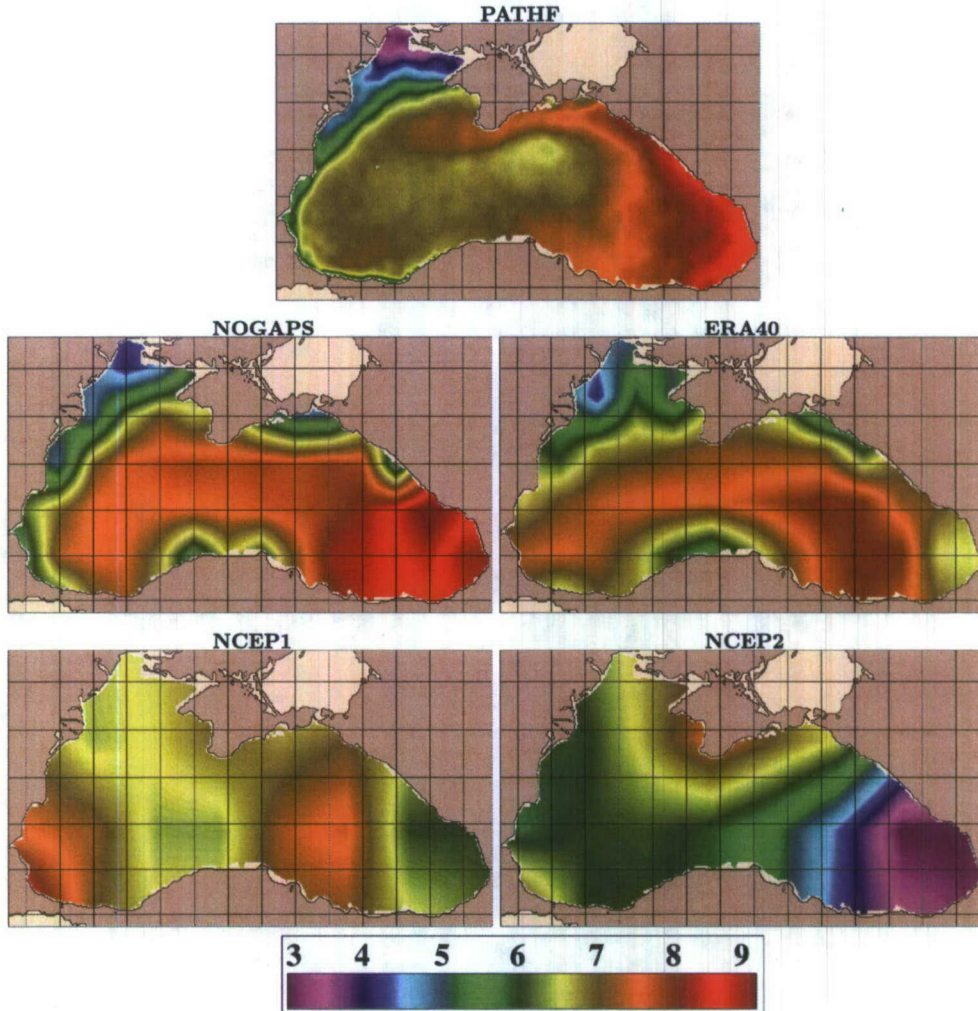


Figure 10. SST climatologies from NWP products in February after applying the creeping sea-fill, as described in the text. The PATHF climatology is also included as a reference data set.

ques, also contribute to the magnitude of values given in Table 6. However, it is the relative rankings of these standard deviations that are important, not their absolute magnitudes, in understanding the performance of the climatologies [Casey and Cornillon, 1999]. The mean differences are not necessarily useful indicators since the various climatologies can have different base periods. However, for climatologies based on similar years, they do provide additional information on the performance.

6. Summary and Conclusions

[47] In this paper, we provide a comprehensive analysis of climatological SST in the Black Sea. Monthly mean SST climatologies formed from a total of eight products are evaluated, in detail. Results reveal that all products agree with each other in the interior quite well. In particular, annual mean SST bias for a given SST product is almost zero in comparison to the finest resolution PATHF climatology. RMS SST difference over the seasonal cycle is typically $<1^{\circ}\text{C}$ and even $\approx 0.5^{\circ}\text{C}$ over most of the Black Sea.

[48] We answer many potential questions as follows: (1) What are the main differences among SST climatologies? SST climatologies from multiple observational- and NWP-based products are obtained or formed. The paper identifies

Table 6. Evaluations of SST Products With In Situ SSTs From ICOADS^a for the Whole Black Sea^b

Climatology	Std. Dev., $^{\circ}\text{C}$	Mean, $^{\circ}\text{C}$
PATHF	2.25	-0.31
NOAA	2.28	-0.38
MODAS	2.26	0.24
WOA01	2.25	-0.46
NOGAPS	2.49	-0.24
ERA40	2.53	-0.96
NCEP1	3.07	-1.70
NCEP2	3.23	-2.49

^aStandard deviation of the SST differences and mean biases for each climatology are calculated with respect to the inter-annual ICOADS data set from 1942 to 2007. See text for details of calculations.

^bAs in Table 5, similar computations were also repeated outside the land-sea mask for NWP products.

different SST errors and demonstrates differences in effectiveness for these products. (2) How do observation-based climatologies differ from the NWP-based ones? Results clearly reveal some accuracy issues in SST near the coastal boundaries. Any researcher needs to be aware of such errors before using SSTs for any type of offshore applications over the sea. The land contamination for SST is discussed for NCEP, ECMWF and NOGAPS, which have different grid resolutions. (3) Can a user have more reliable SSTs from NWP products near the coastal regions? We apply a creeping sea-fill methodology to reduce the land contamination, and form monthly climatologies. The validity, success and deficiencies of the methodology are presented using SSTs from all NWP products. One of the major conclusions is that higher resolution data sets are essential for understanding the variability and climatological conditions in the Black Sea. (4) Does the technique work for different NWP products? Fine resolution satellite-based PATHF climatology (sea-only SST) is processed to check the validity of the approach. It is used as a spatial representation of truth for evaluation of NWP products. We demonstrate the robustness of the technique when applied to NCEP, ECMWF, and NOGAPS. (5) What is the accuracy of each SST product in comparison to in situ observations? We obtained individual historical observations from the ICOADS data set. Overall, the standard deviation around the biases for the observation-based and NWP-based (after the sea-fill) products agree remarkably well.

[49] Major differences between observation- and NWP-based products arise near the coastal boundaries when observation- and model-based ones are compared. This difference is attributed to land contamination of surface soil temperatures from NWP products due to their relatively coarse grid resolutions. Because there is no clear separation between water and land temperatures within a given grid box on the land-sea boundary, SSTs from NWP products typically result in incorrect estimates when representing temperatures over the sea. To overcome this problem a simple algorithm, based on the elimination of land-corrupted atmospheric grid points and replacement by adjacent, purely over-ocean values is applied to original NWP model-based SST values at 6 h time intervals. These new climatologies result in more realistic coastal SSTs for NOGAPS and ERA40 but not for NCEP whose resolution is too coarse for a small ocean basin, such as the Black Sea.

[50] One of main questions is why one would expect SST fields from global atmospheric reanalyses from NWP centers to accurately represent observed SSTs. Whether or not the NWP products were intended to accurately represent SST or could better represent SST if they were run as part of a coupled assimilative air/ocean system, the existing NWP products are typically being used to represent SST, for example, in heat flux calculations for ocean model hindcasts. Our study will help indicate consequences that can be expected from various products including those from NWP centers. We do demonstrate that all NWP products examined in this paper give very accurate SSTs in comparison to observation and satellite-based products in the interior. This is a significant result that is not obvious given the different spatial resolutions, boundary layer parameter-

izations, and data assimilation methods utilized by the different NWP centers.

[51] Finally, discrepancies among SST climatologies also demonstrate potential pitfalls in constructing a climatology in the presence of a trend. If SST data are nonstationary, the differences between different sample intervals can be aliased into a climatological bias. As explained in the paper, this is the case for MODAS in comparison to other observation-based SST products. A similar problem arises within a single data set if the data do not uniformly sample shorter variations.

[52] **Acknowledgments.** We would like to thank H. Hurlburt and J. Metzger of NRL for providing helpful comments. Constructive suggestions made by two anonymous reviewers are appreciated. This work is funded by the Office of Naval Research (ONR) under the 6.2 project, Improved Synthetics Ocean Properties (ISOP). T. Oguz's participation is supported in parts by the EU SESAME and TUBITAK projects. The paper is contribution NRL/JA/7320/07/8016 and has been approved for public release.

References

Barron, C. N., and A. B. Kara (2006), Satellite-based daily SSTs over the global ocean, *Geophys. Res. Lett.*, **33**, L15603, doi:10.1029/2006GL026356.

Bendat, J. S., and A. G. Piersol (2000), *Random Data: Analysis and Measurement Procedures*, 624 pp., John Wiley, New York.

Casey, K. S., and P. Comillon (1999), A comparison of satellite and in situ based sea surface temperature climatologies, *J. Clim.*, **12**, 1848–1863.

Daley, R. (1991), *Atmospheric Data Analysis*, 457 pp., Cambridge Univ. Press, Cambridge, U.K.

Fairall, C. W., E. F. Bradley, J. E. Hare, A. A. Grachev, and J. B. Edson (2003), Bulk parameterization of air-sea fluxes: Updates and verification for the COARE algorithm, *J. Clim.*, **16**, 571–591.

Källberg, P., A. Simmons, S. Uppala, and M. Fuentes (2004), ERA-40 Project Report Series, 17, The ERA-40 archive, 31 pp., Reading, U. K.

Kalnay, E. (1996), The NCEP/NCAR 40-year Re-Analysis Project, *Bull. Am. Meteorol. Soc.*, **77**, 437–471.

Kanamitsu, M., W. Ebisuzaki, J. Woollen, S.-K. Yang, J. J. Hnilo, M. Fiorino, and G. L. Potter (2002), NCEP–DOE AMIP-II Reanalysis (R-2), *Bull. Am. Meteorol. Soc.*, **83**, 1631–1643.

Kara, A. B., and C. N. Barron (2007), Fine-resolution satellite-based daily SSTs over the global ocean, *J. Geophys. Res.*, **112**, C05041, doi:10.1029/2006JC004021.

Kara, A. B., A. J. Wallcraft, and H. E. Hurlburt (2007), A correction for land contamination of atmospheric variables near land-sea boundaries, *J. Phys. Oceanogr.*, **37**, 803–818.

Kilpatrick, K. A., G. P. Podesta, and R. Evans (2001), Overview of the NOAA/NASA Advanced Very High Resolution Radiometer Pathfinder algorithm for sea surface temperature and associated matchup database, *J. Geophys. Res.*, **106**, 9179–9197.

Locarnini, R. A., A. V. Mishonov, J. I. Antonov, T. P. Boyer, and H. E. Garcia (2006), World Ocean Atlas 2005, vol. 1, in *Temperature*, NOAA Atlas NESDIS 61, edited by S. Levitus, 182 pp., U. S. Government Print. Off., Washington, D. C.

May, D. A., M. M. Parmeter, D. S. Olszewski, and B. D. McKenzie (1998), Operational processing of satellite sea surface temperature retrievals at the Naval Oceanographic Office, *Bull. Am. Meteorol. Soc.*, **79**, 397–407.

Oguz, T., T. Cokacar, P. Malanotte-Rizzoli, and H. W. Ducklow (2003), Climatic warming and accompanying changes in the ecological regime of the Black Sea during 1990s, *Global Biogeochem. Cycles*, **17**(3), 1088, doi:10.1029/2003GB002031.

Oguz, T., J. W. Dippner, and Z. Kaymaz (2006), Climatic regulation of the Black Sea hydro-meteorological and ecological properties at interannual-to-decadal time scales, *J. Mar. Syst.*, **60**, 235–254.

Reynolds, R. W., N. A. Rayner, T. M. Smith, D. C. Stokes, and W. Wang (2002), An improved in situ and satellite SST analysis for climate, *J. Clim.*, **15**, 1609–1625.

Rosmond, T. E., T. João, M. Peng, T. F. Hogan, and R. Pauley (2002), Navy Operational Global Atmospheric Prediction System (NOGAPS): Forcing for ocean models, *Oceanography*, **15**, 99–108.

Smith, T. M., and R. W. Reynolds (1998), A high-resolution global sea surface temperature climatology for the 1961–90 base period, *J. Clim.*, **11**, 3320–3323.

Stephens, C., J. I. Antonov, T. P. Boyer, M. E. Conkright, R. A. Locarnini, T. D. O'Brien, and H. E. Garcia (2002), *World Ocean Atlas 2001*, vol. 1, in *Temperature* [CD-ROM], NOAA Atlas NESDIS 49, edited by S. Levitus, 167 pp., U. S. Government Print. Off. Washington, D. C.

Thiebaux, H. J., M. A. Pedder (1987), Spatial objective analysis, in *With Applications in Atmospheric Science*, 299 pp., Elsevier, London.

Worley, S. J., S. D. Woodruff, R. W. Reynolds, S. J. Lubker, and N. Lott (2005), ICOADS Release 2.1 data and products, *Int. J. Climatol.*, 25, 823–842.

C. N. Barron, A. B. Kara, and A. J. Wallcraft, Naval Research Laboratory, Oceanography Division, Code 7320, Building 1009, Stennis Space Center, MS 39529, USA. (birol.kara@nrlssc.navy.mil)

K. S. Casey, NOAA National Oceanographic Data Center, 1315 East West Highway, Silver Spring, MD, 20910, USA. (kenneth.casey@noaa.gov)

T. Oguz, Institute of Marine Sciences, Middle East Technical University, P.O. Box 28, 33731, Erdemli, Icel, Turkey. (oguz@ims.metu.edu.tr)